JOURNAL OF MATERIALS SCIENCE 25 (1990) 661–668

Oxide films formed on aluminium-enriched surfaces of 304 stainless steel in high-temperature water containing Co ions

YOSHIKI OSHIDA
Department of Mechanical and Aerospace Engineering, Syracuse University, Syracuse, New York 13244–1240, USA

Aluminium-enriched surfaces of 18Cr–8Ni stainless steel were subjected to oxidation in 285° C water containing 1 p.p.b. dissolved cobalt for 336 h. Microanalytical studies (scanning electron microscope, X-ray dispersive energy analysis, ion mass spectroanalysis, and ion microprobe mass analysis) were employed to examine the behaviour of cobalt in the oxides formed. It is concluded that (1) the main oxide formed on aluminium-enriched surface is a diaspore, (2) diffusion heat treatment improves the oxidation rate, and (3) the cobalt level decreases constantly from the surface to the interface of the oxide formed on aluminium-enriched samples.

1. Introduction

Metallic materials (mainly AISI Type 304 stainless steel) used in water-cooled nuclear reactors show a higher corrosion rate in high-temperature and high-pressure water under radiation conditions than under non-radiation conditions [1–3]. For example, Mizuno *et al.* [2], studying the effects of γ-ray radiation on iron and cobalt dissolution of 18Cr–8Ni stainless steel, observed that dissolution concentrations of cobalt and iron particles in 250° C water increased as a function of exposure time to radiation and that the dissolution level was approximately three to five times higher than that under non-radiation conditions.

Among radioactivated nuclides (including ^{95}Zr, ^{97}Zr, ^{58}Co, ^{60}Co, ^{65}Ni, ^{51}Cr, ^{59}Fe, ^{54}Mn, ^{56}Mn, ^{99}Mo and ^{101}Mo), which commonly exist in cooling water, ^{60}Co, ^{65}Ni, and ^{59}Fe show the highest γ-energy levels. In addition, ^{60}Co has exceptionally a high half-life (5.26 y), while the latter two nuclides have relatively short half-lives (2.56 h for ^{65}Ni and 45 d for ^{59}Fe) [1, 4, 5]. Consequently, the level of radioactivity due to ^{60}Co in cooling water will continuously increase to cause the so-called ^{60}Co build-up problems.

The level of radiation is an important determinant of not only ^{60}Co build-up but also a susceptibility to the stress corrosion cracking (SCC), as reported by Kuribayashi *et al.* [6]. They examined the SCC susceptibility of sensitized 304 stainless steels in a boiling 12% NaCl solution. It was found that all specimens sensitized between 550 and 800° C were failed due to the intergranular type stress corrosion cracking (IGSCC) under cobalt-radiation conditions after 162 h exposure.

Moreover, Fujita *et al.* [7], studying the effects of γ-ray exposure and dissolved oxygen on the IGSCC susceptibility of the sensitized 304 stainless steel in high-temperature water (250° C), concluded that IGSCC was accelerated by a radiation exposure when the dissolved oxygen concentration is relatively low (i.e. DO $\leqslant$ 20 p.p.b).

Mechanisms of a ^{60}Co build-up phenomenon have been proposed, based on either an incorporation reaction or an exchange reaction of ^{60}Co with oxide films [8]. They are: (i) an incorporation of ^{60}Co into oxide crystal structures as the oxides are formed; (ii) a chemical exchange of cobalt and ^{60}Co for other elements such as nickel; or (iii) an isotopic exchange of radioactive cobalt in reactive water for non-radioactive cobalt in the oxide film. Clearly, reaction (i) is the dominant during the initial exposure of a new or decontaminated surface [8]. Because oxide films can have a significant effect on the long-term ^{60}Co build-up (dose) rate, the long-term ^{60}Co build-up is determined primarily by exchange of ^{60}Co in reactor water with the other element in the oxide film by the exchange reactions (ii) and (iii) [8]. Hence, soluble cobalt is incorporated into the oxide films, so that it will be recognized that the activity build-up rate is highly dependent upon the oxidation rate of stainless steels.

Several processes have been proposed to eliminate or reduce the ^{60}Co build-up problems [1]. They include a control of water chemistry and pre-filming. The pre-filming, for example by chromium, will slow down the initial ^{60}Co build-up; however, in the later stage the growing oxides will incorporate ^{60}Co. In an oxidizing environment, such as a high level of dissolved oxygen water, the protective Cr_2O_3 oxide will be leached out of the film [1]. Hence, the pre-surface treatment should meet the following requirements; (i) the film formed by the pre-surface treatment must be stable in a reactor water environment, and (ii) the film must not be easy to incorporate and/or exchange with ^{60}Co to form a spinel-type oxide including ^{60}Co ions.

It is well known that chromium and aluminium are

0022–2461/90 $03.00 + .12

effective alloying elements to improve the oxidation resistance in ferrous alloys [9], due to the formation of dense and protective sesquioxides such as Cr_2O_3 and Al_2O_3. Moreover, these oxides do not contain divalent ions in their crystal structures, so that they will not exchange with the ^{60}Co. Therefore, Al_2O_3 and Cr_2O_3 are oxides which satisfy the requirements mentioned above. Instead of adding these effective alloying elements, the coating of these elements on the metal surface should provide the same results as far as an oxidation resistance is concerned.

In the present studies, oxides formed on aluminium-enriched surfaces of AISI Type 304 stainless steel were investigated and the effects of aluminium-coating on reducing the ^{60}Co build-up problems will be discussed.

2. Experimental procedure

Three different samples were prepared. A mechanically polished 18Cr-8Ni stainless steel using a metallographic paper (grit 600) was prepared for a control sample A. Sample B was aluminized on the mechanically polished surface. The aluminizing was done by a hot-dipping process (at 700° C for 30 min) by using high-purity aluminium (99.999%). Although it is believed that 3% to 5% of the silicon addition to aluminium for the hot-dipping improves wettability of a molten alloy to the substrate surface [10], after long-term service about at 300 to 500° C, complex intermetallic compounds such as $Fe_2Si_2Al_2$ or Fe_2SiAl_9 will precipitate at the interface between the coated layer and the substrate, resulting in a poor adherency and a continuous crack throughout the coated layer [11]. Hence, a high-purity aluminium without any additive elements was used for an aluminizing. Sample C was a heat-treatment sample B, to obtain a diffusion alloyed layer of iron and aluminium (at 900° C for 1 h).

Samples A, B, and C were suspended within a shroud in a titanium-made autoclave in the closed-loop testing system in the following order: B (at the top) → C → A. The water entered the shroud from the bottom. This test system consists of a 1 litre autoclave with heat exchangers, a reservoir and conditioning tank for controlling the water chemistry, and an analytical loop for monitoring the pH, conductivity and dissolved oxygen concentration of the feed water. To fit the available space of the shroud of 1.25 cm diameter and 10.5 cm long, both side-surfaces of each sample (original dimensions: 29.5 mm × 29.5 mm × 4.5 mm) were machine-cut. Therefore, both side-surfaces of samples B and C revealed their substrate stainless steel layers. Both top and bottom ends of each sample were linked together with stainless steel wire through 3 mm diameter holes in the above sequence. Samples were exposed for 336 h to 285° C deionized water containing 200 ± 20 p.p.b. dissolved oxygen and 1 p.p.b. dissolved cobalt at a flowrate of 200 ml min^{-1}. Cobalt was introduced to the test system as nitrate, $(CoNO_3)_2 \cdot 6H_2O$. The measured pH of the water at 285° C was between 5.65 and 5.70.

Samples after autoclave oxidation tests were examined under the scanning electron microscope (SEM), X-ray dispersive energy analysis (XDA), secondary ion mass spectroanalysis (SIM), and ion microprobe mass analyser (IMMMA) for depth profiles.

3. Results and discussion

Fig. 1 shows the cross-sectional microstructures of samples B and C. The aluminized sample B has an outer surface layer of α-Al_2O_3 of 30 μm, and an Fe–Al diffusion alloy layer of 70 μm thick. An alloyed layer of Fe–Al has a Vicker's hardness number of approximately 500 on average, and is speculated to consist of $FeAl_3$ plus a trace of Fe_2Al_5 (the latter is believed to be a very hard intermediate compound [12–14]). After diffusion heat-treatment, it was observed that the alloyed layer was thickened to 150 μm. In order to remove the surface α-Al_2O_3 layer and an excess aluminium, a vibration, centrifugal, or compressed air method is usually employed. In this study, the excess aluminium and α-Al_2O_3 layer of sample C was removed by a compressed air method.

After autoclave oxidation tests, all of samples gained weight. Sample A showed a weight gain of 0.48 mg

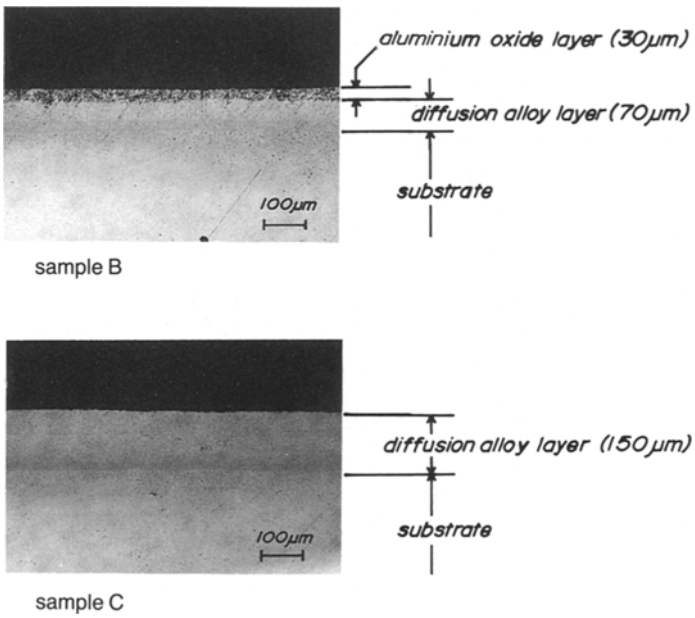

Figure 1 Cross-section microstructures of sample B (aluminized) and sample C (diffusion heat-treated of aluminized sample), substrate: AISI Type 304 stainless steel, ×100.

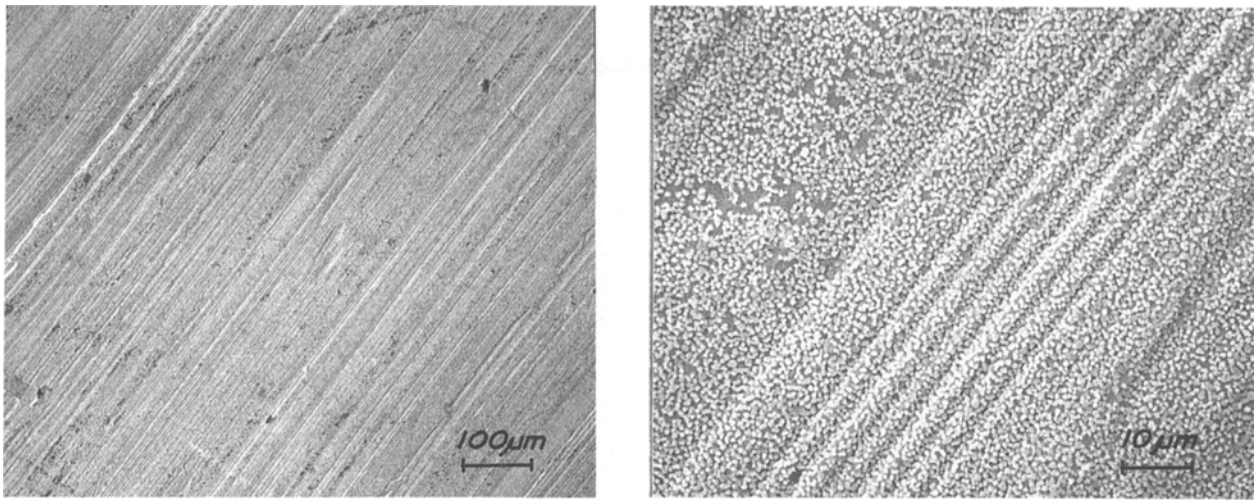

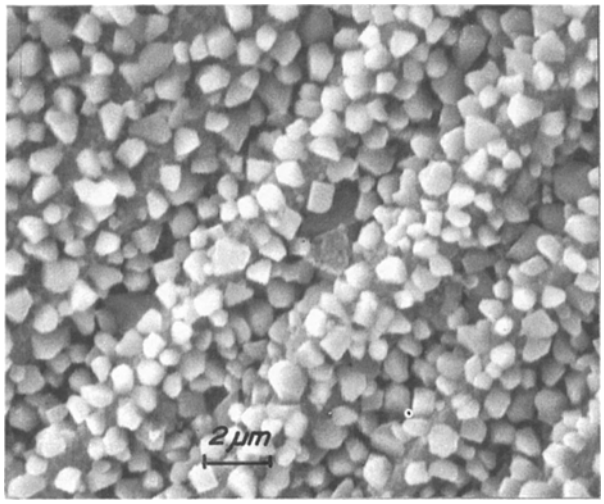

Figure 2 Scanning electron micrographs of sample A (untreated) after the autoclave test (285° C, 336 h).

which is converted to 0.05 mg cm^{-2}. Samples B and C showed weight gains of 23.5 mg (i.e. 3.46 mg cm^{-2}) and 11.6 mg (1.70 mg cm^{-2}), respectively.

Fig. 2 shows the SEM of sample A after an autoclave test. It was observed that equi-size oxide crystals were formed on untreated 304 stainless steel with a somewhat greater density of these crystals along scratch lines caused by mechanical polishing. According to Oshida *et al.* [15–18] and others [19], these oxide crystals will be a mixture of sesqui-oxides and spinel-type oxides. The upper part of Fig. 3 shows SIM results obtained from sample A. The sputtered area was 7.4 × 7.4 μm. It was observed that these oxide

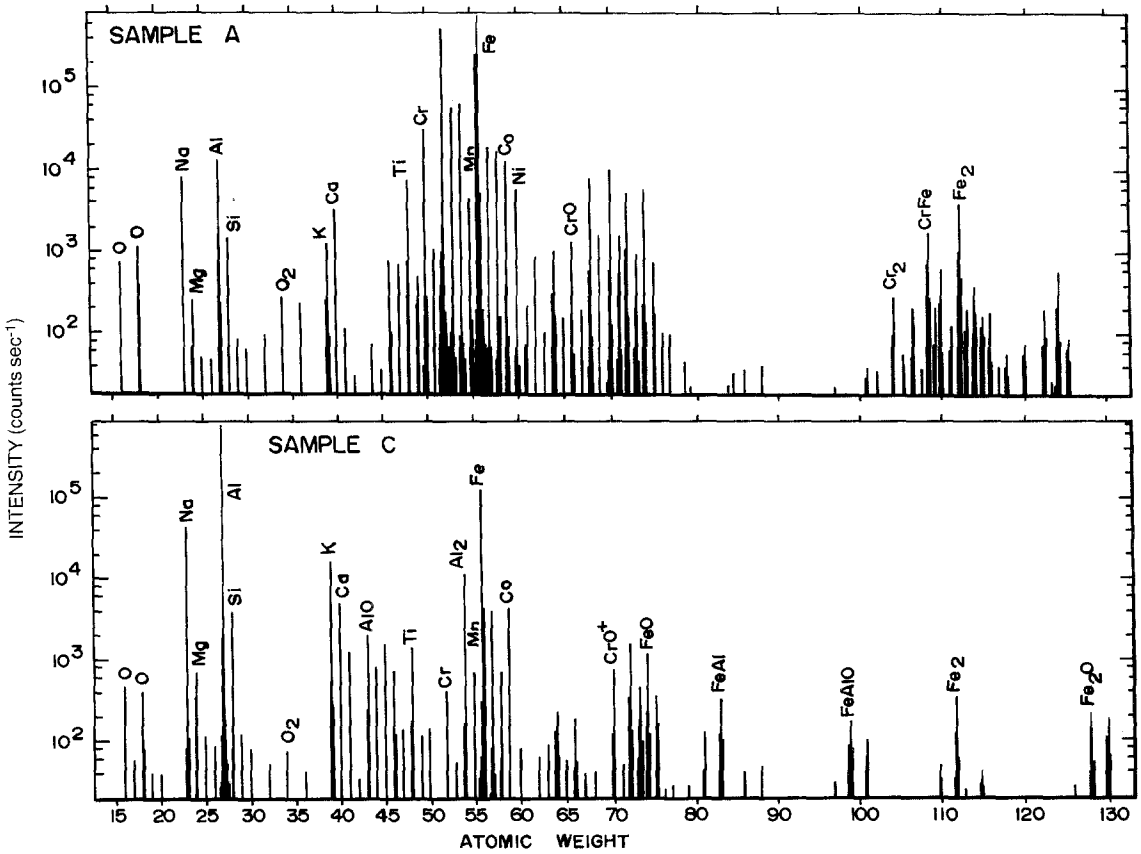

Figure 3 Secondary ion mass spectra of samples A and C.

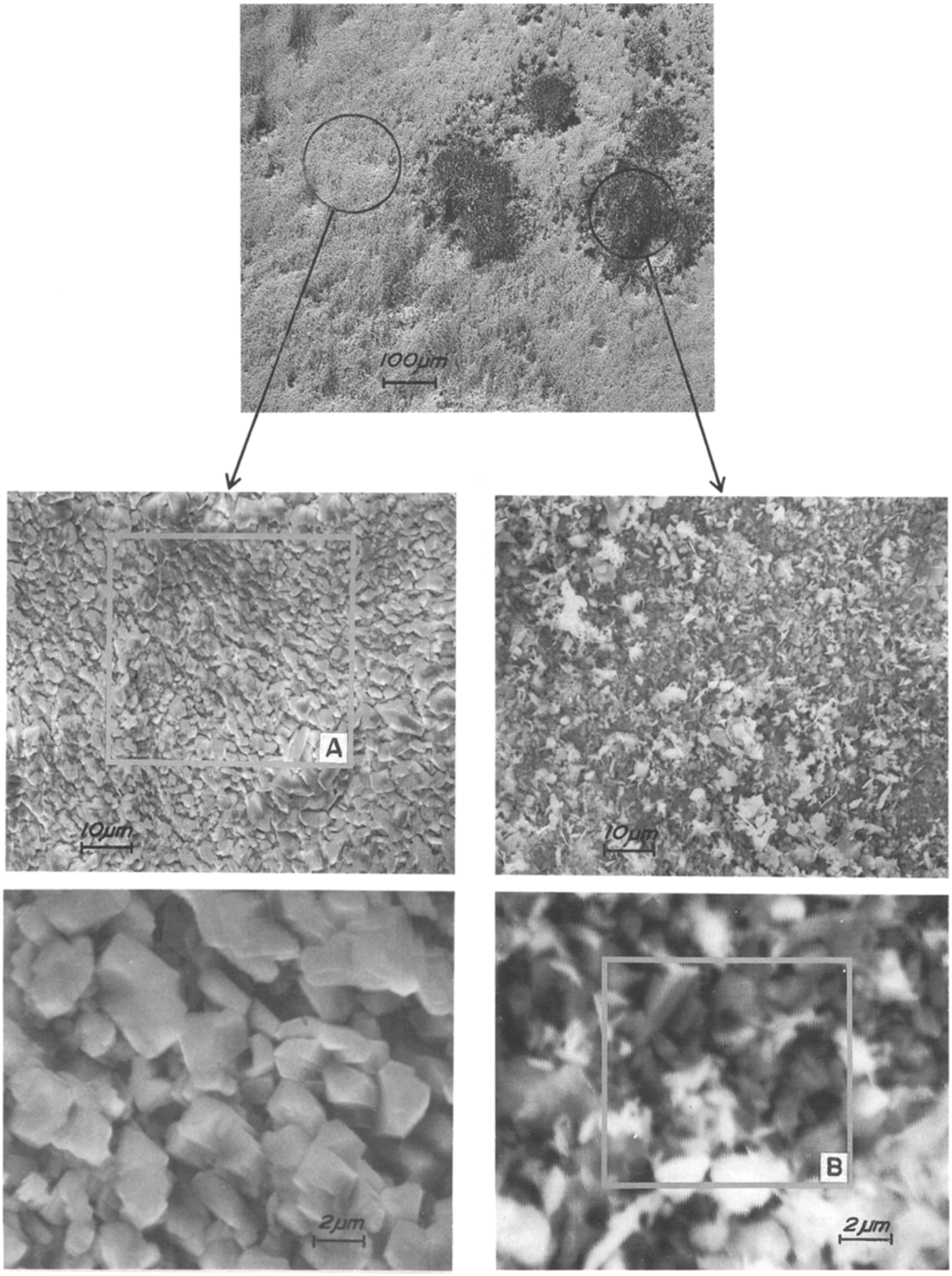

Figure 4 Scanning electron micrographs of sample B (aluminized) after the autoclave test (285° C, 336 h).

crystals contain the main cations of iron, chromium and nickel of 304 stainless steel and also other elements such as titanium, aluminium and cobalt. Titanium may be contaminated from titanium ions dissolved from the autoclave material. Aluminium may be from the other samples, and cobalt comes undoubtedly from a dosed chemical.

Fig. 4 shows SEM structures of sample B. The oxide crystals were larger that those formed on sample A. The XDA results showed that the oxides on sample B were mainly composed of aluminium.

T_M (penetration of aluminium due to oxidation) and T_O (thickness of oxide film) can be related to: $T_M = (MW_M/MW_O)(\varrho_0/\varrho_M)T_O$, where MW_O is the molecular weight and ϱ_O the specific gravity of the oxide, and MW_M and ϱ_M those of the metal [20, 21]. It is generally said that rhombic $Al_2O_3 \cdot H_2O$ is oxide formed on aluminium-enriched surfaces. Therefore,

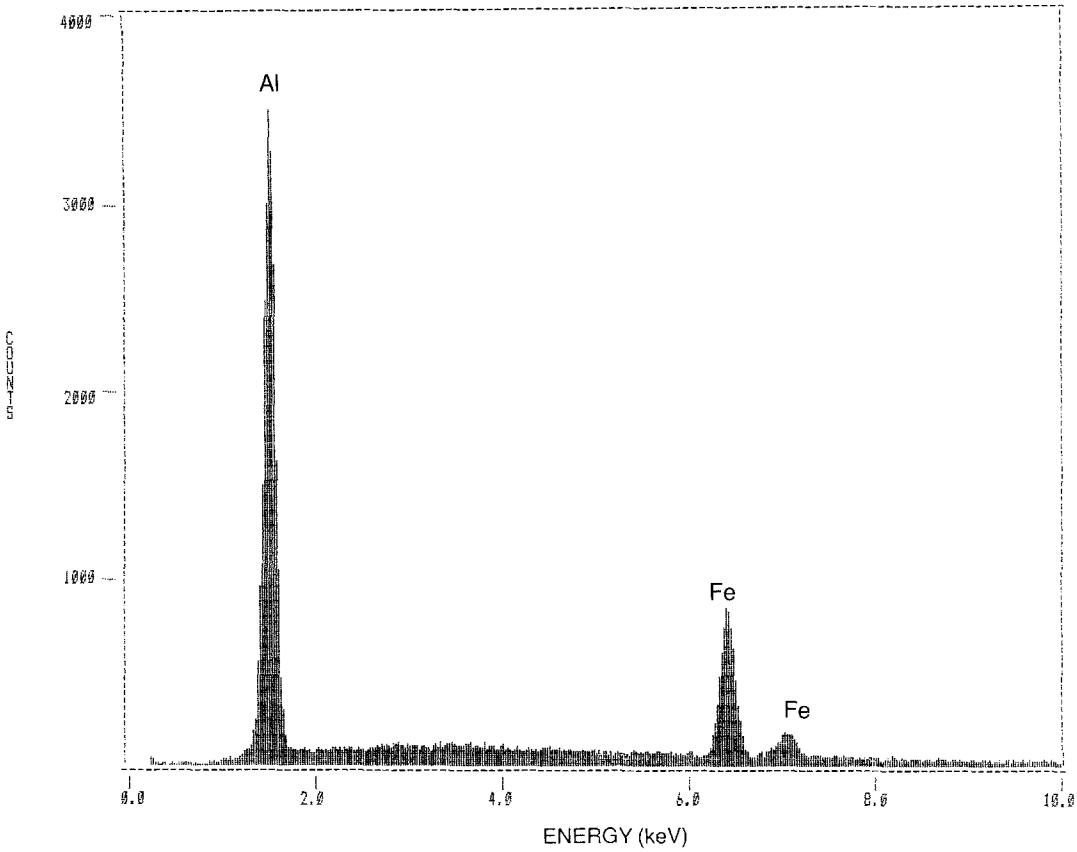

Figure 5 X-ray dispersive analysis at area "b" of sample B shown in Fig. 4.

MW_M = 53.96, MW_O = 119.97, ϱ_M = 2.702, and ϱ_O = 3.014. Then $T_M = 0.502T_O$. This gives the thickness ratio of metal (which is converted to oxide) to oxide film. The measured total weight gain (ΔW_T) is a result of ΔW_O (oxide weight gain) minus ΔW_M (metal ion loss). It can be said that, from Fig. 4 (left-hand side), that the oxide film thickness is about 8 to 10 crystal layers deep; i.e. T_O = 16 to 20 μm thick. Hence, the total weight gain per unit surface area = $\varrho_O T_O - \varrho_M T_M$ = 2.65 to 3.32 mg cm^{-2}. These numbers are in reasonable agreement with the calculated weight gain/unit surface area (3.46 mg cm^{-2}), and agree fairly well with results reported by Greenblatt and McMillan [22].

On the other hand, the dark area, B, in Fig. 4 shows different oxide features than those formed in area A. The oxides formed seem to consist of a uniform oxide layer as in area A and whisker-type oxides. According to XDA analysis (Fig. 5), area B contains mainly aluminium plus a small amount of iron. These chunks or whiskers of the oxide could be diaspore needles [23]. These oxides seems to be a similar type of oxide to that formed on sample C, as shown Fig. 6.

Fig. 7 shows scanning electron micrographs of the oxidized side surface (which was machine-cut) and oxidized surface of the diffusion heat-treated surface. Referring to the XDA results shown in Fig. 8, spot "c" indicates that the surface oxide formed on untreated 18Cr–8Ni stainless steel consists of iron, chromium and nickel. The XDA results on spot "a" indicate that the oxides are the same as those formed on sample B, i.e. they consist of mainly aluminium cations. The surface of sample C, prior to high-temperature water oxidation, was a solid solution of iron and aluminium. Under an autoclave test, aluminium was selectivity oxidized. SIM analysis on oxides formed on sample C is shown in the lower part of Fig. 3. A strong intensity of aluminium was observed. In addition, the initial stage of the surface oxide film such as (Fe, Al)O as well as the substrate material (Fe, Al) and cobalt, were observed.

Fig. 9 shows IMMA depth profiles of the main elements of interest (iron, chromium, nickel, cobalt, aluminium, titanium and oxygen), which comprise the oxides formed on sample A. Fig. 9a shows the intensities of each element in terms of counts per second and Fig. 9b shows the intensity ratio of each element to that of iron. Both are plotted as a function of sputter time as well as distance from the surface. The sputtered area was 65 μm × 65 μm and the sputter rate was 0.110 nm sec^{-1}. Although, due to the uneven nature of the oxide, "islands" of oxide undoubtedly remain in the crater region, the metal substrate had been reached after 0.2 μm depth sputtering. It should be noted that the ratio of iron to cobalt inside the oxides seems to be constant. Cobalt build-up for the (Fe, Ni)O · (Fe, Cr)$_2$O$_3$/Co system for sample A can be explained by either incorporation with iron cations or cation exchange of cobalt ions with metal ions in the already formed oxides, as mentioned previously [8].

Fig. 10 shows IMMA depth profiles of oxides formed on sample C. Note that analysis conditions were changed before and after the depth from the surface was about 0.25 μm. Of interest is that the Fe/Co intensity ratio seems to decrease continuously as a function of distance from the surface. Making the same argument as before, $T_M = 0.502T_O$ and the observed weight gain/unit area = 1.70 mg cm^{-2}, then

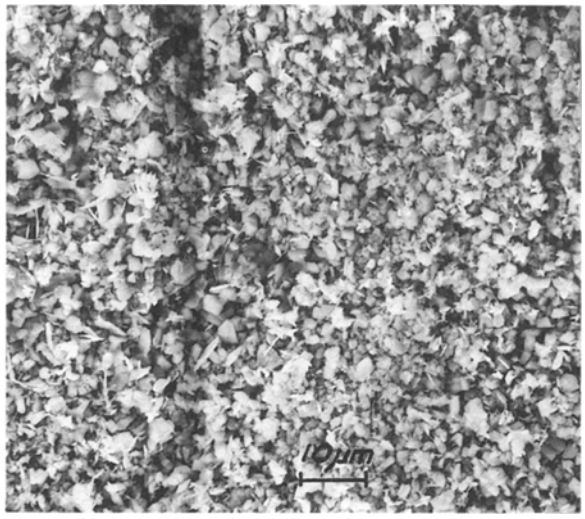

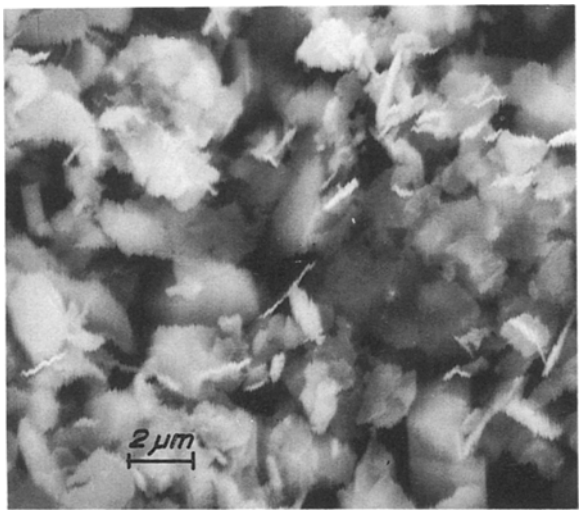

Figure 6 Scanning electron micrographs of sample C (diffusion heat-treated) after the autoclave test (285° C, 336 h).

$\Delta W = 3.014T_O - 2.702T_O = 1.658T_O$. Hence the estimated surface oxide thickness, T_O, will be of the order of 1 to 2 μm. By comparison of the intensity ratios of Fe/Co for both samples A and C, it indicates that the aluminium-enriched layer seems to reduce the cobalt level inside the surface layer rather than the untreated surface substrate.

Although there are extensive data available on the stability of aluminium oxides, the results are not consistent. For example, the transition temperature from bayerite ($Al_2O_3 \cdot 3H_2O$) to diaspore ($Al_2O_3 \cdot H_2O$) is reported at 80 to 85° C [24, 25], 55 to 110° C [26], 150° C [27], or 200° C [28]. Moreover, the dehydration temperature from diaspore to alumina is reported at 100 to 300° C [29], or 380° C [28]. As discussed previously, the results of weight change suggested that the oxide films formed on an aluminium-enriched surface after 285° C water oxidation for 336 h will be identified as a diaspore. For an $Al_2O_3 \cdot H_2O$/Co system, because a divalent cobalt ion is hardly incorporated with a diaspore or is difficult to exchange with the Al^{3+} ion, it is speculated that cobalt may be a contamination between each diaspore crystal. A further investigation is needed to understand this point fully.

4. Conclusions

Aluminium-enrichments were employed on AISI type stainless steel prior to oxidation in 285° C water containing 1 p.p.b. dissolved cobalt for 336 h. The main conclusions drawn from a limited number of experimental data are as follows.

1. The main oxide formed on aluminium-enriched surfaces is suggested to be a diaspore, according to weight change calculations.
2. The oxidation rate of a diffusion heat-treated aluminium-coated surface was approximately half that observed from the aluminized surface.
3. The Fe/Co ratio within the oxide formed on untreated surfaces is constant, while it decreases continuously from the surface to the interface of the oxide formed on aluminium-enriched samples.
4. Although the state of the cobalt ion found in the diaspore is not clearly understood, surface coating with aluminium on stainless steel will reduce the cobalt dose level.

Acknowledgements

The author thanks Mr L. W. Niedrach and Dr H. A. Storms, General Electric Co., for their extensive preparative assistance for autoclave oxidation tests and microanalysis, and Mr A. Ohshima, Shinko Kinzoku Co., for preparation of aluminium coating on 304 stainless steels.

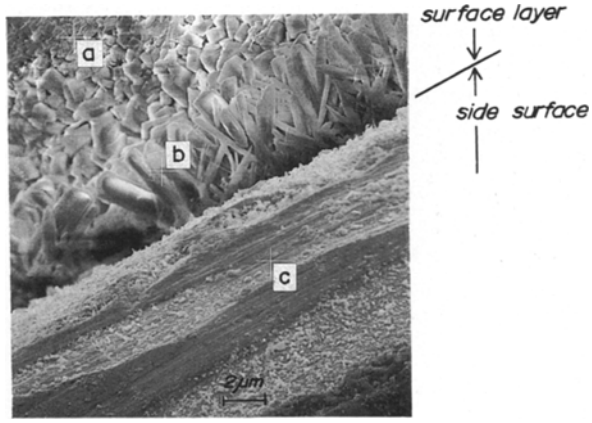

Figure 7 Scanning electron micrograph at a corner portion of sample C after the autoclave test (285° C, 336 h).

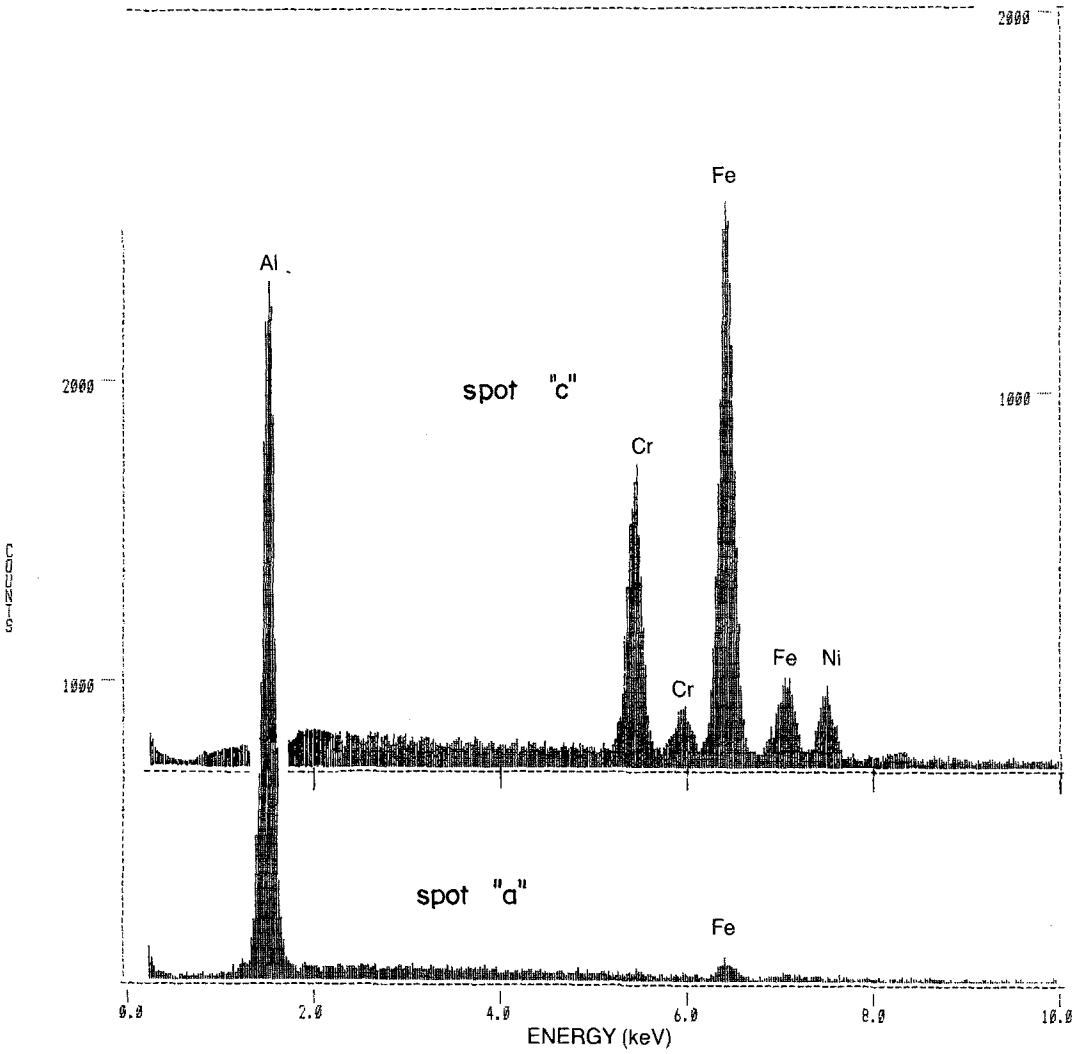

Figure 8 X-ray dispersive analyses at spots "a" and "c" of sample C, shown in Fig. 7.

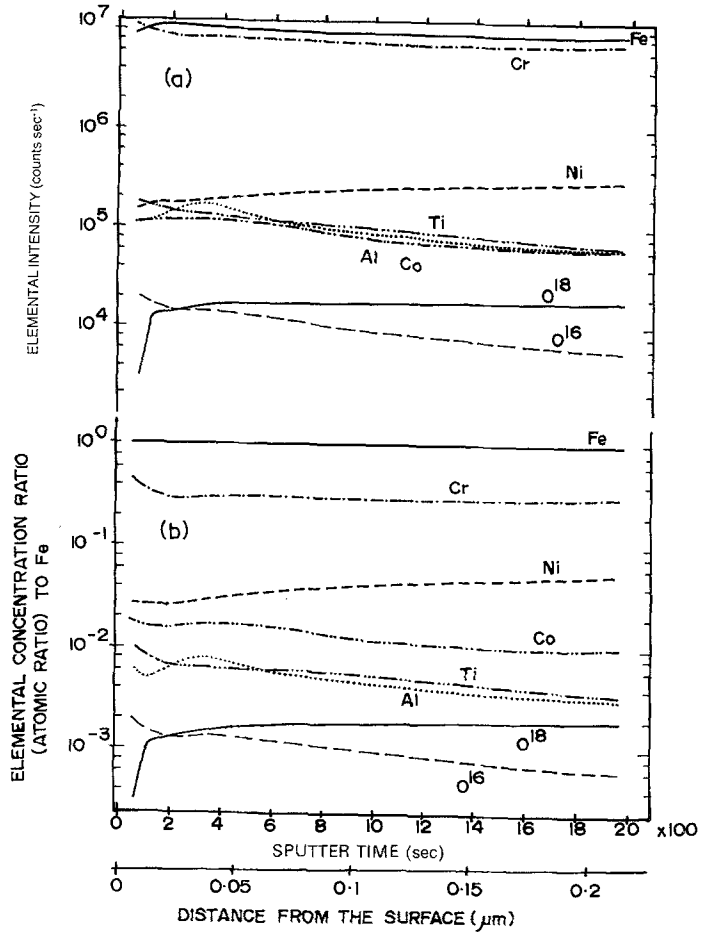

Figure 9 IMMA depth profile of sample A: (a) elemental intensity plotted against sputter time or distance from the surface, and (b) elemental concentration ratio (atom ratio) to iron plotted against sputter time or distance from the surface.

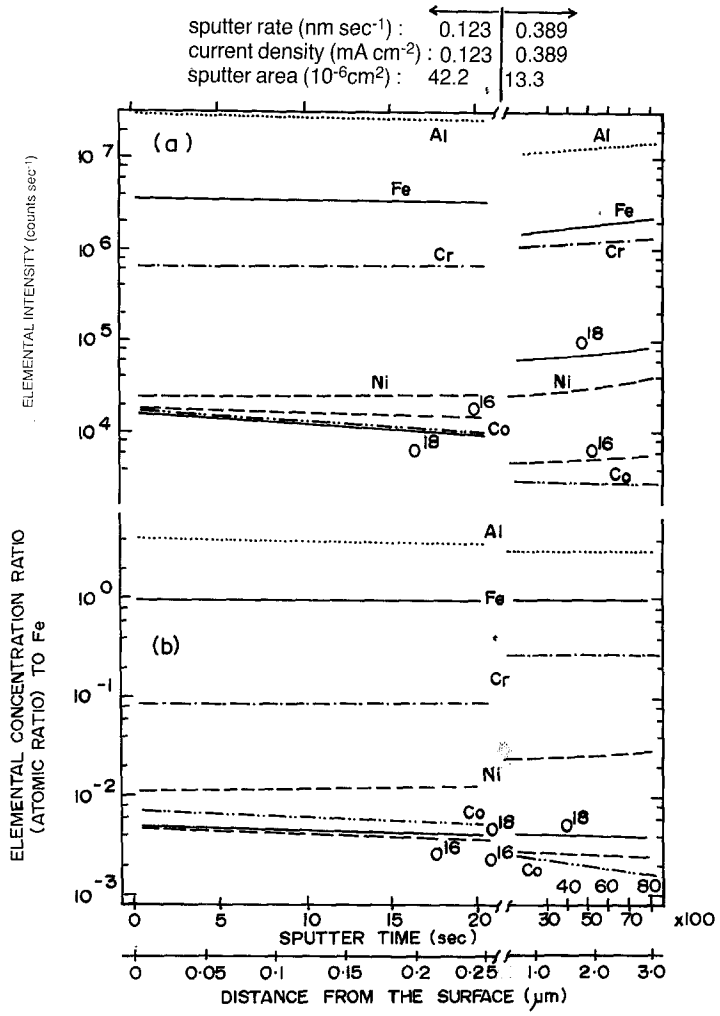

Figure 10 IMMA depth profiles of sample C: (a) elemental intensity plotted against sputter time or distance from the surface, and (b) elemental concentration ratio (atom ratio) to iron plotted against sputter time or distance from the surface.

References

1. W. E. BERRY and R. B. DIEGLE, "Survey of Corrosion Product Generation, Transport, and Deposition in Light Water Nuclear Reactors", EPRI Final Report NP-522 (1979).
2. S. MIZUNO *et al.*, Proceedings of the 25th Meeting on Corrosion and Protection (1978) p. 57 (in Japanese).
3. K. SHIMOGORI, *Materials* **35** (1980) 1085 (in Japanese).
4. P. J. GRANT, A. J. KENNEDY, D. F. HALLMAN, E. T. CHULICK and D. L. UHL, "Oconee Radiochemistry Survey Program", Babcock and Wilcox Report RDTPL 75-4 (1975).
5. J. E. LESURF, Proceedings of the EPRI System Contamination Workshop (1975) p. 197.
6. M. KURIBAYASHI *et al.*, Proceedings of the Spring Meeting of the Japan Institute of Metals (1979) p. 136 (in Japanese).
7. N. FUJITA, M. AKIYAMA and T. TAMURA, *Corrosion* **37** (1981) 335.
8. L. D. ANSTINE, "BWR Radiation Assessment and Control (BRAC)", Final Report, EPRI NP-3114 (1979).
9. N. D. TOMASHOV, "Theory of Corrosion and Protection of Metals" (MacMillan, New York, 1966) p. 102.
10. K. TAGAYA, M. ISA and O. TANI, *J. Metal Surface Technol.* **10** (1959) 363.
11. Y. OSHIDA, unpublished report.
12. H. KOSUGE and H. TAKADA, *Light Metals* **29** (1979) 64.
13. E. GEBHARDT and W. OBROWSKI, *Z. Metallkde* **44** (1953) 154.
14. G. GUERTLER and K. SAGEL, *ibid.* **46** (1955) 738.
15. T. NAKAYAMA, Y. OSHIDA and T. IKEZAWA, "On the Oxide Film Formed on Stainless Steels in Deaerated High Temperature Water", The Castings Research Lab. Report, Waseda University, no. 21 (1970) p. 9.
16. Y. OSHIDA and T. NAKAYAMA, *Jpn Inst. Metals* **35** (1971) 1108.
17. T. NAKAYAMA and Y. OSHIDA, *Trans. Jpn Inst. Metals* **11** (1970) 245.
18. *Idem*, *Corrosion* **24** (1962) 336.
19. J. M. FRANCIS and W. H. WHITLOW, *J. Nucl. Mater.* **20** (1966) 1.
20. J. H. GREENBLATT, *Corrosion* **19** (1963) 295.
21. R. L. DILLON and H. C. BOWEN, *ibid.* **18** (1962) 406.
22. J. H. GREENBLATT and A. F. McMILLAN, *ibid.* **19** (1963) 146.
23. U. R. EVANS, "The Corrosion and Oxidation of Metals", First Supplementary Volume (St. Martins Press, New York, 1968) p. 183.
24. G. ITOH, "Corrosion Science and Technology" (Corona, 1977) p. 251.
25. Y. YAMAZAKI and H. HARIMOTO, *J. Metal Finishing Soc. Jpn* **20** (1969) 59.
26. J. C. GRIESS, H. C. SAVAGE, T. H. MAUNEY, J. L. ENGLISH and J. G. RAINWATER, "Effect of Heat Flux on the Corrosion of Al by Water", Oak Ridge National Laboratory, ORNL-3056 (February 1961).
27. D. D. MACDONALD and P. BUTLER, *Corr. Sci.* **13** (1973) 259.
28. F. J. SHIPKO and R. M. HAGG, KAPL Report 1740 (1957).
29. M. I. TSYPIN, I. L. ROSENFELD, YU. P. OL'KHOVNOKOV and S. V. VIZHEKHOVSKAYA, "A Study of the Corrosion of Aluminum in High Temperature Water", (California, 1967) p. 230.

Received 11 October 1988
and accepted 7 April 1989